Tensor Communication Waveform Design With Semi-Blind Receiver in the MIMO System

Zheng Dou, *Member, IEEE*, Chunmei Li, Chao Li, Xiao Gao, and Lin Qi

***Abstract*—A flexible mathematical framework for adaptive wireless communication waveform design is of importance for the implement of the cognitive radio-based software defined radio (CR-based SDR). As one of the popular models, the "spectrally modulated spectrally encoded" (SMSE) was proposed to tackle this problem but it cannot be trivially applied to the (massive) multiple input multiple output (MIMO) systems. In this paper, we extend the useful SMSE model into MIMO systems. Inspired by the *tensor* technique in signal processing and machine learning, we reformulate the desired waveforms as a higher-order tensors, of which the modes correspond to various modulation parameters such as coding chips, frequency and antennas. Beside the waveform design model, we further propose a new semi-blind receiver for the new model. Due the uniqueness of the applied tensor decomposition, we proved that the proposed receiver can jointly estimate the user symbols and channel state information without the aid of pilot sequences. Experimental results demonstrate the effectiveness of the proposed model in various communication scenes and outperforms the baseline systems. approximately 3 dB compared with the ideal receiver.**

***Index Terms*—Waveform design, semi-blind receiver, multiple input multiple output (MIMO) system, PARAFAC model, TUCKER-1 model.**

I. Introduction

COGNITIVE radio (CR) is an extension of software defined radio (SDR) [1]. It is widely used in military and commercial communications such as next generation networks [2], dynamic spectrum access [3], the IEEE 802.22 standard [4], and multiple input multiple output (MIMO) systems [5]. MIMO has been regarded as a promising technology for the next-generation wireless communications [6]. As shown in Fig. 1, a typical cognitive cycle is composed of four aspects: spectrum sensing, spectrum analysis, spectrum decision, and waveform framework. Spectrum decision determines the reconfigurable parameters such as data rate, operating frequency, modulation mode, and transmission power, according to the results acquired by spectrum sensing and analysis. The CR network adapts the communication waveforms to the wireless environment by changing these reconfigurable parameters [7]. Therefore, it is of great significance to construct a waveform design framework to characterize communication waveforms by these reconfigurable parameters in the CR system.

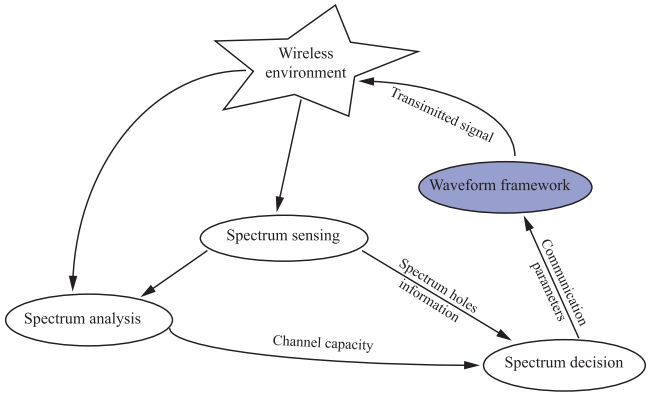

Fig. 1. A typical cognitive radio cycle.

A. Dynamic Waveform Design Models

Spectrally modulated, spectrally encoded (SMSE) framework can be utilized successfully in the CR system as part of the waveform framework [8]. It can be applied to controling power, such as the plan proposed by [9] and [10]. Hao Huang implements the neural network to beamforming design which can achieve the performance comparable to traditional algorithms but with lower complexity [11]. Jinlong Sun uses the BiLSTM to deal with the problem of RF power amplifiers distortion [12]. These algorithms need a unified model for parameter configuration. This is because SMSE is constructed with six kinds of waveform design variables representing different characteristics of the multi-carrier waveform. By changing the variables, the SMSE framework can generate different kinds of waveforms, enabling it to operate as the generation framework for the CR-based SDR platform. However, SMSE can not generate communication waveforms suitable for the MIMO system because it has a larger gain of diversities and multiplexing than the traditional single antenna system. Therefore, it is necessary to extend the SMSE framework to the MIMO system.

In 2007, M. L. Roberts proposed a general framework for analyzing, characterizing, and implementing SMSE signals within

Manuscript received June 4, 2019; revised September 19, 2019 and November 18, 2019; accepted November 18, 2019. Date of publication December 13, 2019; date of current version February 12, 2020. This work was supported in part by the National Natural Science Foundation of China (61671167 and 61671154), in part by the Fundamental Research Funds for the Central Universities (HEUCFG201830), and in part by the International Exchange Program of Harbin Engineering University for Innovation-oriented Talents Cultivation. The review of this article was coordinated by Prof. G. Gui. *(Corresponding author: Lin Qi.)*

Z. Dou, C. Li, X. Gao, and L. Qi are with the Department of Information and Communication Engineering, Harbin Engineering University, Harbin 150000, China (e-mail: douzheng@hrbeu.edu.cn; lichunmei_heu@outlook.com; 525731012@hrbeu.edu.cn; qilin@hrbeu.edu.cn).

C. Li was with Harbin Engineering University, Harbin 150000, China. He is now with RIKEN Center on Advanced Intelligence Project, Tokyo 103-0027, Japan (e-mail: chao.li@riken.jp).

Digital Object Identifier 10.1109/TVT.2019.2958402

CR-based SDR architecture [8]. It was the first framework to describe communication waveforms by several parameters, and was used to solve the problem of coexistence [13], [14] and interference suppression [15], [16]. The extended framework soft decision SMSE (SD-SMSE) can simultaneously generate overlay and underlay waveforms by adjusting the parameters so it can be applied in dynamic spectrum access (DSA) technology [17], [18]. R. Zhou then demonstrated that the SMSE and SD-SMSE framework can be matched successfully in a SDR platform [19]. Y. Zhao added a new spatial variable to the SMSE framework and changed the dimension of the variables to make SMSE more suitable for the MIMO system [20]. However, it was not a serious analytical framework and very complicated. Z. Dou proposed a tensor modulated tensor encoded (TMTE) framework which introduced tensor algebra to the extension of the SMSE framework [21]. But the method was only suitable for binary phase shift keying (BPSK) modulation and lacked flexibility. The TMTE framework brings a new method of tensor algebra to construct communication waveform framework and it has the flexibility to generate different kinds of waveforms.

B. Tensor Decomposition Model in Communication Systems

The tensor decomposition model is a new method to solve communication problems. A tensor is a multidimensional array which can be viewed as a high-order extension of a matrix that can handle a huge amount of data. Tensor decompositions can be applied in numerous fields, including psychometrics, chemometrics, numerical linear algebra, computer vision, numerical analysis, data mining, neuroscience, and graph analysis [22]. Tensor decompositions can also be used in wireless communication systems to model the received signal and establish a direct association among the physical parameters of the communication link [23]. A MIMO system requires at least two dimensions such as space-time and space-frequency. Additionally, three or more dimensions such as space-time-frequency-code are required to represent the received signals. At this time, the multi-dimensional nature of tensors can be utilized to construct the received signals in a MIMO system so that it can benefit from the multiple forms of diversity.

This research [24], [25] makes use of tensor decomposition models to design new space-time-frequency coding methods and blind receivers in a MIMO system. Tensor decompositions can also be applied in a MIMO relay system to model the transmitted and received signals [26], [27]. Moreover, some tensor decomposition models have the features of identifiability and uniqueness in the case of satisfying certain conditions. These performances can be used to blindly/semi-blindly recover symbols and estimate/equalize channel information without using long training sequences [28], [29], [30]. There are numerous other applications in wireless communication for tensor decompositions, such as direction-of-arrival (DOA) estimation for massive MIMO systems [31], noisy compressive sampling (CS) based on block-sparse tensors [32], the deep learning structure [33], packet routing strategy [34], multi-dimensional spectrum map construction [35] and more [36], [37], [38]. Such diverse application in wireless communication illustrates that the tensor is an excellent tool to solve numerous wireless communication problems.

C. Contributions

This paper presents a new tensor communication waveform design framework by tensor decomposition models to extend the SMSE framework to a MIMO system. The two typical tensor decomposition models PARAFAC [39] and TUCKER-1 [40] provide the mathematical basis of the proposed framework. The specific operation is to substitute the core tensor of the TUCKER-1 model to the PARAFAC decomposition. The proposed model can achieve the function of generating different kinds of multi-carrier waveforms in a MIMO system by adjusting the component matrices, which are also called variables. A new semi-blind receiver is also proposed in this paper to recover user symbols and estimate channel information based on the alternating least square (ALS) algorithm. The effectiveness of the communication system will be improved because the new semi-blind receiver does not require pilot sequences to estimate the channel state information. Few sequences are required by the receiver to eliminate ambiguities. Compared to the SMSE framework, the contributions of this paper are summarized as follows:

i) The proposed framework can generate different kinds of multi-carrier waveforms which are well-suited for the MIMO system, and the configuration of the variables is more flexible than SMSE;

ii) The proposed semi-blind ALS receiver can achieve the function of a joint semi-blind symbol recovery and channel estimation without using pilot sequences.

The remainder of the paper is organized as follows: In Section II, a brief overview of PARAFAC and TUCKER-1 models is provided. The variables and the proposed model is formulated in Section III, and in Section IV, identifiability and uniqueness issues are discussed. A semi-blind ALS receiver is presented for joint channel estimation and symbol detection in Section V. A selection of simulation results are the provided in Section VI to illustrate the performance of the proposed framework and the semi-blind receiver. Finally, conclusions are discussed in Section VII.

II. Preliminary

The basis of the proposed framework presented in this paper is SMSE. A brief introduction of the mathematical SMSE framework is thus provided. Furthermore, PARAFAC and TUCKER-1 are key elements of the proposed framework. The particular description and formulation can be found in [22]. Some important concepts are provided here to aid in the understanding of the proposed model, and the mathematical models are detailed as follows.

Notations: In this paper, blackboard bold letters are used to denote the real and complex domains, e.g., $\mathbb{R}$, and $\mathbb{C}$. Scalars are denoted by italic letters, e.g., m, N, and vectors are represented by boldface lowercase capitals, e.g., $\mathbf{a}, \mathbf{b}$. Matrices are denoted

by boldface uppercase, e.g., $\mathbf{A}, \mathbf{B}$, and tensors are described by copperplate letters, e.g., $\mathcal{A}, \mathcal{B}$. Subscripts $\mathbf{A}^{\mathrm{T}}$ and $\mathbf{A}^{\dagger}$ stand for transpose and pseudo-inverse of $\mathbf{A}$, respectively. The horizontal, lateral, and frontal slices of a 3rd-order tensor $\mathcal{X} \in \mathbb{C}^{I_1 \times I_2 \times I_3}$, is denoted respectively by $\mathcal{X}_{i_1 \cdot \cdot}, \mathcal{X}_{\cdot i_2 \cdot}, \mathcal{X}_{\cdot \cdot i_3}$. Subscripts $\mathbf{a}_{\cdot n}$ and $\mathbf{a}_{m \cdot}$ represent the n-th column and the m-th row of the matrix $\mathbf{A} \in \mathbb{R}^{M \times N}$, respectively, and $diag(\mathbf{a}_{\cdot n})$ is used to denote the diagonal matrix, which is composed of the n-th column of matrix $\mathbf{A} \in \mathbb{R}^{M \times N}$. In addition, $\|\cdot\|_{\mathrm{F}}$ denotes Frobenius norm, and $\circ$, $\otimes$, $\diamond$, and $\odot$ are the outer product, Kronecker product, Khatri-Rao product, and Hadamard product, respectively. The relationship between the Kronecker product and Khatri-Rao product is denoted by:

$$\begin{aligned}\mathbf{A} \diamond \mathbf{B} &= [\mathbf{a}_{\cdot 1} \otimes \mathbf{b}_{\cdot 1}, \ldots, \mathbf{a}_{\cdot R} \otimes \mathbf{b}_{\cdot R}] \\ &= \begin{bmatrix} \mathbf{B} diag(\mathbf{a}_{1 \cdot}) \\ \mathbf{B} diag(\mathbf{a}_{2 \cdot}) \\ \vdots \\ \mathbf{B} diag(\mathbf{a}_{R \cdot}) \end{bmatrix} \in \mathbb{C}^{I_1 I_2 \times R} \end{aligned} \tag{1}$$

where $\mathbf{A} = [\mathbf{a}_{\cdot 1}, \ldots, \mathbf{a}_{\cdot R}] \in \mathbb{C}^{I_1 \times R}$, $\mathbf{B} = [\mathbf{b}_{\cdot 1}, \ldots, \mathbf{b}_{\cdot R}] \in \mathbb{C}^{I_2 \times R}$.

A. SMSE Framework

SMSE framework is the basis of the tensor model proposed in this paper. The spectral mathematical model of SMSE can be represented by $\mathbf{X} = \mathbf{A} \odot \mathbf{\Theta} \odot \mathbf{F}$, where $\mathbf{A}$, $\mathbf{\Theta}$, and $\mathbf{F}$ denote the amplitude, phase, and frequency, respectively. They are the function of six waveform design variables which are assigned frequency ($\mathbf{a}$), used frequency ($\mathbf{u}$), data modulation ($\mathbf{d}$), code ($\mathbf{c}$), window ($\mathbf{w}$), and orthogonality ($\mathbf{o}$), respectively. The SMSE framework can be denoted in the form of six waveform design variables according to:

$$\begin{aligned} x_n[f] = a_f u_f d_{f,n} c_f w_f \\ e^{j(\theta_{d_{f,n}} + \theta_{c_f} + \theta_{w_f} + \theta_{o_{f,n}})} \end{aligned} \tag{2}$$

where $x_n[f]$ is the f-th frequency of the n-th SMSE symbol. Assuming that there are a total of F frequencies in the system, a_f and u_f are the elements of the assigned frequency $\mathbf{a} = [a_1, a_2, \ldots, a_F] \in \{0,1\}^{1 \times F}$ and the used frequency $\mathbf{u} = [u_1, u_2, \ldots, u_F] \in \{0,1\}^{1 \times F}$, which both denote the allocation of frequencies. While $\mathbf{a}$ represents the system assigning a subset of F frequencies to a user, the actual used frequency of the user is denoted by $\mathbf{u}$ due to interference or other circumstances. It should be noted that the values of the two frequency allocation variables are 0's and 1's. The system does not assign the frequency to a user when $a_f = 0$, and the user can not use the frequency when $u_f = 0$. Subscripts $d_{f,n}, \theta_{d_{f,n}}, c_f, \theta_{c_f}, w_f, \theta_{w_f}$ and $\theta_{o_{f,n}}$ are the corresponding amplitudes and phases of the waveform design variables. $d_{f,n} e^{j\theta_{d_{f,n}}}$ denotes the modulation method of each SMSE symbol in a certain frequency, which is an entry of the data modulation variable $\mathbf{d} = [d_1, d_2, \ldots, d_F] \in \mathbb{C}^{1 \times F}$. In addition, $c_f e^{j\theta_{c_f}}$ and $w_f e^{j\theta_{w_f}}$ are the elements of the code variable $\mathbf{c} = [c_1, c_2, \ldots, c_F] \in \mathbb{C}^{1 \times F}$ and the window variable $\mathbf{w} = [w_1, w_2, \ldots, w_F] \in \mathbb{C}^{1 \times F}$, respectively. They denote the coding method and windowing function of the transmitted signal in the frequency domain. The last term $\theta_{o_{f,n}}$ belongs to the phase-only orthogonality variable $\mathbf{o}$ which is represented by $\mathbf{o} = [o_1, o_2, \ldots, o_F] \in \mathbb{C}^{1 \times F}$ and $|\mathbf{o}_f| = 1$ for all f. In this paper, we reformulate the communication waveforms as higher-order tensor instead of the conventional matrix form. Below, we will briefly recall two popular tensor decomposition models that is used in our model.

TABLE I
WAVEFORM DESIGN VARIABLES OF THE SMSE FRAMEWORK

Parameter	Meaning	Value
$\mathbf{a}$	Assigned frequency	$\mathbf{a} = [a_1, a_2, \cdots, a_F] \in \{0,1\}^{1 \times F}$
$\mathbf{u}$	Used frequency	$\mathbf{u} = [u_1, u_2, \cdots, u_F] \in \{0,1\}^{1 \times F}$
$\mathbf{d}$	Data modulation	$\mathbf{d} = [d_1, d_2, \cdots, d_F] \in \mathbb{C}^{1 \times F}$
$\mathbf{c}$	Code	$\mathbf{c} = [c_1, c_2, \cdots, c_F] \in \mathbb{C}^{1 \times F}$
$\mathbf{w}$	Window	$\mathbf{w} = [w_1, w_2, \cdots, w_F] \in \mathbb{C}^{1 \times F}$
$\mathbf{o}$	Orthogonality	$\mathbf{o} = [o_1, o_2, \cdots, o_F] \in \mathbb{C}^{1 \times F}$

B. PARAFAC Model

The PARAFAC decomposition model of tensor can be used in space-time frequency coding, so it can be used as an extension way of SMSE model. The PARAFAC decomposition factorizes a tensor into a sum of rank-one tensors. The specific formulation of the 3rd-order tensor $\mathcal{X} \in \mathbb{C}^{I \times J \times K}$ can be denoted in the form of the outer products of vectors by

$$\mathcal{X} = \sum_{r=1}^{R} \mathbf{a}_{\cdot r} \circ \mathbf{b}_{\cdot r} \circ \mathbf{c}_{\cdot r} + \mathcal{E} \tag{3}$$

where R denotes a positive integer, $\mathbf{A} = [\mathbf{a}_{\cdot 1}, \mathbf{a}_{\cdot 2}, \ldots, \mathbf{a}_{\cdot R}] \in \mathbb{C}^{I \times R}$, $\mathbf{B} = [\mathbf{b}_{\cdot 1}, \mathbf{b}_{\cdot 2}, \ldots, \mathbf{b}_{\cdot R}] \in \mathbb{C}^{J \times R}$, and $\mathbf{C} = [\mathbf{c}_{\cdot 1}, \mathbf{c}_{\cdot 2}, \ldots, \mathbf{c}_{\cdot R}] \in \mathbb{C}^{K \times R}$ are three component matrices, and $\mathcal{E} \in \mathbb{C}^{I \times J \times K}$ is the error tensor. The equivalent scalar form is denoted by:

$$x_{i,j,k} = \sum_{r=1}^{R} a_{i,r} b_{j,r} c_{k,r} + e_{i,j,k} \tag{4}$$

where $a_{i,r}$, $b_{j,r}$, and $c_{k,r}$ are the elements of the component matrices $\mathbf{A} \in \mathbb{C}^{I \times R}$, $\mathbf{B} \in \mathbb{C}^{J \times R}$, and $\mathbf{C} \in \mathbb{C}^{K \times R}$, respectively, and $e_{i,j,k}$ is an element of the error tensor $\mathcal{E} \in \mathbb{C}^{I \times J \times K}$.

The 3rd-order PARAFAC decomposition model can also be represented using frontal, lateral and horizontal slices as follows:

$$\begin{aligned} \mathcal{X}_{\cdot \cdot k} &= \mathbf{A} diag(\mathbf{c}_{k \cdot}) \mathbf{B}^{\mathrm{T}} \in \mathbb{C}^{I \times J} \\ \mathcal{X}_{\cdot j \cdot} &= \mathbf{C} diag(\mathbf{b}_{j \cdot}) \mathbf{A}^{\mathrm{T}} \in \mathbb{C}^{K \times I} \\ \mathcal{X}_{i \cdot \cdot} &= \mathbf{B} diag(\mathbf{a}_{i \cdot}) \mathbf{C}^{\mathrm{T}} \in \mathbb{C}^{J \times K} \end{aligned} \tag{5}$$

The tensor unfolding along the n-th mode can then be interpreted as a result of the three slices arranged in different ways. In this paper, the three unfolding forms of a 3rd-order tensor

$\mathcal{X} \in \mathbb{C}^{I\times J\times K}$ can be represented by:

$$\mathbf{X}_1 = \begin{bmatrix} \mathcal{X}_{\cdot\cdot 1} \\ \mathcal{X}_{\cdot\cdot 2} \\ \vdots \\ \mathcal{X}_{\cdot\cdot K} \end{bmatrix} \in \mathbb{C}^{IK\times J}, \mathbf{X}_2 = \begin{bmatrix} \mathcal{X}_{\cdot 1\cdot}^{\mathrm{T}} \\ \mathcal{X}_{\cdot 2\cdot}^{\mathrm{T}} \\ \vdots \\ \mathcal{X}_{\cdot J\cdot}^{\mathrm{T}} \end{bmatrix} \in \mathbb{C}^{KJ\times I},$$

$$\mathbf{X}_3 = \begin{bmatrix} \mathcal{X}_{1\cdot\cdot} \\ \mathcal{X}_{2\cdot\cdot} \\ \vdots \\ \mathcal{X}_{I\cdot\cdot} \end{bmatrix} \in \mathbb{C}^{JI\times K} \tag{6}$$

C. TUCKER-1 Model

Tucker decomposition of tensor is similar to the received tensor signal of the proposed model. This section starts with an introduction to the Tucker decomposition. Tucker-3 decomposition is carried out to decompose the tensor into a core tensor multiplied by a matrix along each mode. The TUCKER-3 decomposition of a 3rd-order tensor $\mathcal{X} \in \mathbb{C}^{I\times J\times K}$ can be represented by:

$$\begin{aligned} \mathcal{X} &= \mathcal{G} \times_1 \mathbf{A} \times_2 \mathbf{B} \times_3 \mathbf{C} + \mathcal{E} \\ &= \sum_{m=1}^{M}\sum_{n=1}^{N}\sum_{r=1}^{R} g_{m,n,r}\left(\mathbf{a}_{\cdot m} \circ \mathbf{b}_{\cdot n} \circ \mathbf{c}_{\cdot r}\right) + \mathcal{E} \end{aligned} \tag{7}$$

where $\times_n$ denotes that a tensor multiplies a matrix along the n-th mode, $\{M, N, R\}$ are three positive indices which satisfy $\{M, N, R\} \ll \{I, J, K\}$, and $g_{m,n,r}$ is the element of the tensor $\mathcal{G} \in \mathbb{C}^{M\times N\times R}$ which is the core tensor of the TUCKER-3 model. The three component matrices are $\mathbf{A} \in \mathbb{C}^{I\times M}$, $\mathbf{B} \in \mathbb{C}^{J\times N}$ and $\mathbf{C} \in \mathbb{C}^{K\times R}$, and the equivalent element-wise form is denoted by:

$$x_{i,j,k} = \sum_{m=1}^{M}\sum_{n=1}^{N}\sum_{r=1}^{R} g_{m,n,r}a_{i,m}b_{j,n}c_{k,r} + e_{i,j,k} \tag{8}$$

It is worth noting that PARAFAC is a specified form of TUCKER-3 in which a diagonal core tensor is set and the main diagonal is composed of 1' s. The TUCKER-1 model is a special case of the TUCKER-3 model, in which only one component matrix $\mathbf{A} \in \mathbb{C}^{I\times M}$ exists, which can be represented as:

$$x_{i,j,k} = \sum_{m=1}^{M} g_{m,j,k}a_{i,m} + e_{i,j,k} \tag{9}$$

where $g_{m,j,k}$ is the entry of the core tensor $\mathcal{G} \in \mathbb{C}^{M\times J\times K}$.

III. Proposed Model

To achieve the objective of extending the SMSE framework, a new tensor communication waveform design framework is presented in this section. The new framework is mainly inspired by the PARAFAC and TUCKER-1 decomposition models as detailed in Section II. In total there are four waveform design variables in the proposed framework. Different kinds of multicarrier waveforms can be obtained by changing the corresponding waveform design variables.

A. Variables

In this section, a MIMO wireless communication system is considered, as illustrated in Fig. 2, The transmitter is equipped with M antennas, the receiver is equipped with K antennas, and the MIMO channel fading matrix is denoted by $\mathbf{H}$. It is assumed that the system can accommodate R users, and the length of each user symbol is N. The new framework can allocate the user symbol $\mathbf{S}$ to different transmitting antennas $\mathbf{A}$ after frequency encoding $\mathbf{C}$ and frequency assignation $\mathbf{U}$. Then, the user symbols can be demodulated by the ideal receiver. The receiver is considered ideal when the channel, frequency encoding, frequency assignation, and antenna allocation matrices are all known by the receiver.

There are four kinds of waveform design variables in the proposed framework. A new antenna allocation variable is introduced to denote the allocation between the user symbols and transmitting antennas. For simplicity and clarity in the proposed framework, the variables of window function and phase-only orthogonality term are not considered in the SMSE framework. The window function can be omitted here because it will not significantly change the form of transmitted waveforms, but changes the shape of the waveform. The phase-only orthogonality term is used in multiple access which is not considered in this circumstance. The variable assigned frequency and used frequency in SMSE both denote the allocation of the frequency. This is always of great importance in a DSA system, so the differences between them are not distinguished in the proposed framework. In the SMSE framework, the variables are denoted by vectors, however, in the proposed framework, the vector-based variables are expanded into a form of matrices. This operation will mean the variables contain more useful information and the form of matrices is more suitable for the tensor models than vectors.

The n-th symbol of the transmitted signal in the proposed framework is represented by:

$$\mathcal{X}_{\cdot\cdot n} = \mathbf{A}diag(\mathbf{s}_{n\cdot})(\mathbf{U} \odot \mathbf{C}) \tag{10}$$

where $\mathcal{X}_{\cdot\cdot n}$ can be interpreted as a frontal slice of the transmitted signal tensor $\mathcal{X}$, $diag(\mathbf{s}_{n\cdot})$ denotes a diagonal matrix formed by $\mathbf{s}_{n\cdot}$, and $\mathbf{s}_{n\cdot}$ is the n-th row of $\mathbf{S}$. From the formulation, the four variables of the proposed framework are data modulation matrix $\mathbf{S} \in \mathbb{C}^{N\times R}$, frequency encoding matrix $\mathbf{C} \in \mathbb{C}^{R\times F}$, frequency assignation matrix $\mathbf{U} \in \{0, 1\}^{R\times F}$, and antenna allocation matrix $\mathbf{A} \in \{0, 1\}^{M\times R}$, respectively.

The data modulation matrix $\mathbf{S} = [\mathbf{s}_{\cdot 1}, \ldots, \mathbf{s}_{\cdot R}]^{R\times N}$ is composed of $N \times R$ symbols, and the symbol $s_{n,r}$ is drawn from the PSK/QAM alphabet. Each user symbol is denoted by a column of the data modulation matrix $\mathbf{s}_{\cdot r}$. Each user's own modulation method is fixed, but can be different from each other. The vector $\mathbf{c}_{r\cdot}$ of frequency encoding matrix $\mathbf{C} = [\mathbf{c}_{1\cdot}, \ldots, \mathbf{c}_{R\cdot}]^{\mathrm{T}} \in \mathbb{C}^{R\times F}$ determines the coding method for every user in the frequency domain. As an examples, orthogonal frequency division multiplexing (OFDM)/multicarrier code division multiple access (MC-CDMA) signals are obtained by choosing the specific values of the variable. When the values of the frequency encoding matrix are '1's, OFDM signals can be acquired. However, for

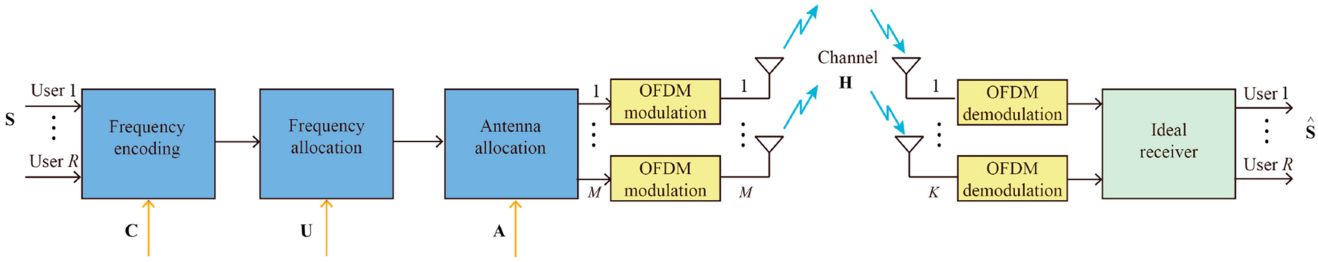

Fig. 2. Implementation of the proposed framework in a MIMO system. The transmitting waveform is constructed by the four waveform design variables which are data modulation matrix $\mathbf{S}$, frequency assignation matrix $\mathbf{U}$, frequency encoding matrix $\mathbf{C}$, and antenna allocation matrix $\mathbf{A}$. The $\mathbf{H}$ denotes the MIMO channel fading matrix, the output $\hat{\mathbf{S}}$ is the symbol recovery matrix by the ideal receiver, and R, M, and K denote the number of users, transmitting antennas, and receiving antennas, respectively.

the MC-CDMA waveform '1's and '-1's must be chosen to compose the frequency encoding matrix. Which frequency that can be used is defined by the frequency assignation matrix $\mathbf{U} = [\mathbf{u}_{1\cdot}, \ldots, \mathbf{u}_{R\cdot}]^{\mathrm{T}} \in \{0,1\}^{R\times F}$. The element $u_{r,f}$ is composed of '0' or '1,' where '0' illustrates that the f-th frequency slot can't be used by the r-th user, while '1' indicates the frequency is assigned. The dimension of the frequency encoding matrix is identical to the frequency assignation counterpart. The antenna allocation matrix $\mathbf{A} = [\mathbf{a}_{\cdot 1}, \ldots, \mathbf{a}_{\cdot R}] \in \{0,1\}^{M\times R}$ is a spatial variable which determines the way for transmitting user symbols by multiple antennas. The dimension of the matrix is $M \times R$, and the values of an element $a_{m,r}$ in this matrix are chosen from '0's and '1's, where '0' illustrates that the m-th antenna will not transmit the r-th user's information.

B. Signal Model: Transmitter

In the transmitter, accounting for all the waveform design variables, the user symbol information denoted by data modulation matrix $\mathbf{S}$ is encoded by frequency encoding matrix $\mathbf{C}$ and frequency assignation matrix $\mathbf{U}$, then allocated by antenna allocation matrix $\mathbf{A}$. Through these operations, the transmitted signal can be obtained. The matrix form of the n-symbol of the transmitted signal is provided in Eq. 10. To understand the generation of the transmitted signal more clearly, the element-wise form $x_{m,f,n}$ of the transmitted signal is included. The n-th symbols that are transmitted by the f-th frequency and the m-th antenna are denoted by:

$$x_{m,f,n} = \sum_{r=1}^{R} a_{m,r} u_{r,f} c_{r,f} s_{n,r} \tag{11}$$

where $r = 1, \ldots, R$, $m = 1, \ldots, M$, $f = 1, \ldots, F$, and $n = 1, \ldots, N$ respectively denote the number of users, transmitting antennas, frequencies and the length of user symbols. Subscripts $a_{m,r}$, $u_{r,f}$, $c_{r,f}$, and $s_{n,r}$ are the elements of matrix $\mathbf{A} \in \{0,1\}^{M\times R}$, $\mathbf{U} \in \{0,1\}^{R\times F}$, $\mathbf{C} \in \mathbb{C}^{R\times F}$, and $\mathbf{S} \in \mathbb{C}^{N\times R}$, respectively.

The tensor form of the transmitted signal can be obtained by using the outer product of vectors. This form illustrates the generation of every user's signal in the proposed framework. Tensor form is familiar with the PARAFAC decomposition model, so the form of the transmitted signal $\mathcal{X} \in \mathbb{C}^{M\times F\times N}$ can

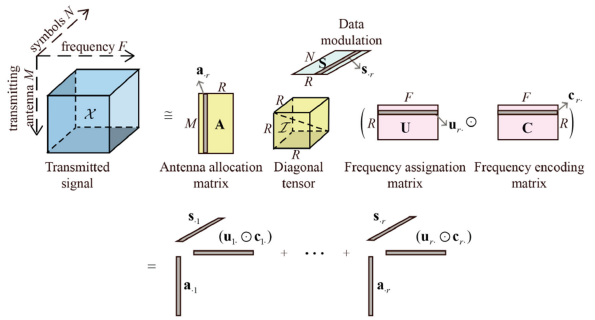

Fig. 3. Formation of the transmitted signal by the proposed framework.

TABLE II
WAVEFORM DESIGN VARIABLES OF THE PROPOSED FRAMEWORK

Parameter	Meaning	Value
$\mathbf{S}$	Data modulation	$\mathbf{S} = [\mathbf{s}_{\cdot 1}, \cdots, \mathbf{s}_{\cdot R}] \in \mathbb{C}^{N\times R}$
$\mathbf{C}$	Frequency encoding	$\mathbf{C} = [\mathbf{c}_{1\cdot}, \cdots, \mathbf{c}_{R\cdot}]^{\mathrm{T}} \in \mathbb{C}^{R\times F}$
$\mathbf{U}$	Frequency assignation	$\mathbf{U} = [\mathbf{u}_{1\cdot}, \cdots, \mathbf{u}_{R\cdot}]^{\mathrm{T}} \in \{0,1\}^{R\times F}$
$\mathbf{A}$	Antenna allocation	$\mathbf{A} = [\mathbf{a}_{\cdot 1}, \cdots, \mathbf{a}_{\cdot R}] \in \{0,1\}^{M\times R}$

be given by:

$$\mathcal{X} = \sum_{r=1}^{R} \mathbf{a}_{\cdot r} \circ (\mathbf{u}_{r\cdot} \odot \mathbf{c}_{r\cdot}) \circ \mathbf{s}_{\cdot r} \tag{12}$$

where $\mathbf{s}_{\cdot r}$ is the r-th column of the data modulation matrix $\mathbf{S} \in \mathbb{C}^{N\times R}$ which represents the modulation method of the r-th user symbol. The r-th row of the frequency assignation matrix $\mathbf{U} \in \{0,1\}^{R\times F}$ is $\mathbf{u}_{r\cdot}$, and the frequency encoding matrix $\mathbf{C} \in \mathbb{C}^{R\times F}$ is $\mathbf{c}_{r\cdot}$, denoting the frequency allocation and encoding of the r-th user. Subscript $\mathbf{a}_{\cdot r}$ is the r-th column of the antenna allocation matrix $\mathbf{A} \in \{0,1\}^{M\times R}$. This vector determines which antenna can be used by the r-th user. Fig. 3 illustrates the formation of the transmitted signal by the proposed framework, and $\mathcal{I}$ represents a diagonal tensor which is composed of 1's.

C. Signal Model: Receiver

To model the received signal, a MIMO channel information matrix denoted by $\mathbf{H} \in \mathbb{C}^{K\times M}$ is considered. The element $h_{k,m}$ of the channel matrix represents the fading coefficients between the m-th transmitting antenna and the k-th receiving antenna.

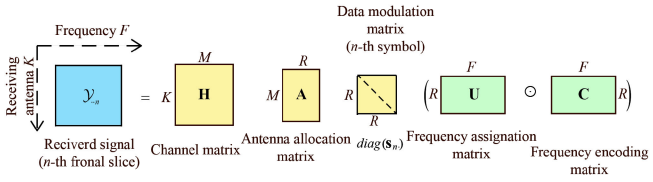

Fig. 4. Generation of the n-th symbol of the received signal in the form of a frontal slice by the proposed framework.

In the following sections of the paper, only the time-invariant and flat fading channel is considered. Therefore, the element $y_{k,f,n}$ of the received tensor signal $\mathcal{Y} \in \mathbb{C}^{K\times F\times N}$ can be represented by Eq. 13 without noise.

$$\begin{aligned} y_{k,f,n} &= \sum_{m=1}^{M} h_{k,m} x_{m,f,n} \\ &= \sum_{m=1}^{M} h_{k,m} \sum_{r=1}^{R} a_{m,r} u_{r,f} c_{r,f} s_{n,r} \\ &= \sum_{m=1}^{M} \sum_{r=1}^{R} h_{k,m} a_{m,r} u_{r,f} c_{r,f} s_{n,r} \end{aligned} \tag{13}$$

where $k = 1, \ldots, K$ denotes the number of receiving antennas, and $y_{k,f,n}$ represents the n-th symbol which transmitted by f-th frequency and received by the k-th antenna. It can be observed that Eq. 13 is familiar with the model of TUCKER-1 decomposition, except that the core tensor of TUCKER-1 is decomposed into PARAFAC.

The n-th received symbol $\mathcal{Y}_{\cdot\cdot n}$ of the received signal can be given by:

$$\mathcal{Y}_{\cdot\cdot n} = \mathbf{H}\mathbf{A} diag(\mathbf{s}_{n\cdot})(\mathbf{U} \odot \mathbf{C}) \tag{14}$$

in which $\mathcal{Y}_{\cdot\cdot n}$ is the frontal slice of the received signal tensor $\mathcal{Y}$. This kind of formulation is necessary for recovering user symbols. The generation of the n-th symbol of the received tensor signal $\mathcal{Y} \in \mathbb{C}^{K\times F\times N}$ is illustrated in Fig. 3.

An ideal receiver is used to recover the user symbols denoted by data modulation matrix $\mathbf{S}$. The ideal receiver is considered one that already knows the channel information matrix $\mathbf{H}$, the frequency assignation matrix $\mathbf{U}$, the frequency encoding matrix $\mathbf{C}$, and the antenna allocation matrix $\mathbf{A}$. Here $\mathbf{Q} = \mathbf{H}\mathbf{A} \in \mathbb{C}^{K\times R}$ and $\mathbf{P} = (\mathbf{U} \odot \mathbf{C})^{\mathrm{T}} \in \mathbb{C}^{F\times R}$, and $\mathbf{q}_{k\cdot}$ denotes the k-th row of the matrix $\mathbf{Q}$. According to Eq. 6, an unfolding form of the received signal tensor can be obtained:

$$\begin{aligned} \mathbf{Y}_3 &= \begin{bmatrix} \mathcal{Y}_{1\cdot\cdot} \\ \mathcal{Y}_{2\cdot\cdot} \\ \vdots \\ \mathcal{Y}_{K\cdot\cdot} \end{bmatrix} = \begin{bmatrix} \mathbf{P} diag(\mathbf{q}_{1\cdot}) \\ \mathbf{P} diag(\mathbf{q}_{2\cdot}) \\ \vdots \\ \mathbf{P} diag(\mathbf{q}_{K\cdot}) \end{bmatrix} \mathbf{S}^{\mathrm{T}} \\ &= ((\mathbf{H}\mathbf{A}) \diamond (\mathbf{U} \odot \mathbf{C})^{\mathrm{T}})\mathbf{S}^{\mathrm{T}} \in \mathbb{C}^{KF\times N} \end{aligned} \tag{15}$$

Noise is not considered in this theoretical model, but it can not be avoided in the actual system. Noise is denoted by $\mathcal{N} \in \mathbb{C}^{K\times F\times N}$, the received signal with noise is represented by $\widetilde{\mathcal{Y}} = \mathcal{Y} + \mathcal{N}$, and the unfolding form of the actual system is given by $\widetilde{\mathbf{Y}}_3$. Therefore, when $KF > R$, user symbols can be recovered by:

$$\hat{\mathbf{S}}^{\mathrm{T}} = ((\mathbf{H}\mathbf{A}) \diamond (\mathbf{U} \odot \mathbf{C})^{\mathrm{T}})^{\dagger} \widetilde{\mathbf{Y}}_3 \tag{16}$$

where $\hat{\mathbf{S}}$ denotes the user symbols recovered by the ideal receiver. Using Eq. 16, the user symbols can be successfully recovered by the ideal receiver.

IV. Semi-Blind ALS Receiver

In this section, a semi-blind receiver is put forward for the proposed model based on the alternating least squares (ALS) algorithm. The ALS is a classical algorithm used to estimate the component matrices of PARAFAC tensor decomposition. Compared to the ideal receiver, the proposed semi-blind receiver does not know the channel information. Furthermore, the semi-blind receiver can recover the user symbol information and channel state information without using pilot sequences, which can be used to increase the information rate. To recover the user symbols $\mathbf{S}$ and channel state information $\mathbf{H}$, another unfolding matrix besides $\mathbf{Y}_2 \in \mathbb{C}^{FN\times K}$ is required, which is $\mathbf{Y}_3 \in \mathbb{C}^{FK\times R}$, and is given in Eq. 17.

$$\begin{aligned} \mathbf{Y}_2 &= \begin{bmatrix} \mathcal{Y}_{\cdot 1\cdot}^{\mathrm{T}} \\ \mathcal{Y}_{\cdot 2\cdot}^{\mathrm{T}} \\ \vdots \\ \mathcal{Y}_{\cdot F\cdot}^{\mathrm{T}} \end{bmatrix} = \begin{bmatrix} \mathbf{S} diag(\mathbf{p}_{1\cdot}) \\ \mathbf{S} diag(\mathbf{p}_{2\cdot}) \\ \vdots \\ \mathbf{S} diag(\mathbf{p}_{F\cdot}) \end{bmatrix} (\mathbf{H}\mathbf{A})^{\mathrm{T}} \\ &= ((\mathbf{U} \odot \mathbf{C})^{\mathrm{T}} \diamond \mathbf{S})\mathbf{A}^{\mathrm{T}}\mathbf{H}^{\mathrm{T}} \in \mathbb{C}^{FN\times K} \end{aligned} \tag{17}$$

where $\mathbf{P} = (\mathbf{U} \odot \mathbf{C})^{\mathrm{T}} \in \mathbb{C}^{F\times R}$ and $\mathbf{p}_{f\cdot}$ denotes the f-th row of the matrix $\mathbf{P}$. It is assumed here that the methods of antenna allocation and frequency assignation are known, meaning the values of matrices $\mathbf{A}$ and $\mathbf{U}$ are known. The values of the frequency encoding matrix $\mathbf{C}$ are also known by the receiver. The target of the proposed semi-blind ALS receiver algorithm is to alternately compute and update the values of the data modulation matrix $\mathbf{S}$ and the channel matrix $\mathbf{H}$ until the recovered matrices satisfy the stopping condition. According to Eq. 15 and Eq. 17, the semi-blind ALS receiver can be represented by:

$$\hat{\mathbf{S}}_i^{\mathrm{T}} = ((\mathbf{H}\mathbf{A}) \diamond (\mathbf{U} \odot \mathbf{C})^{\mathrm{T}})^{\dagger} \widetilde{\mathbf{Y}}_3 \tag{18}$$

$$\hat{\mathbf{H}}_i^{\mathrm{T}} = \left(\left((\mathbf{U} \odot \mathbf{C})^{\mathrm{T}} \diamond \mathbf{S}\right)\mathbf{A}^{\mathrm{T}}\right)^{\dagger} \widetilde{\mathbf{Y}}_2 \tag{19}$$

where i denotes the iteration number. Specifically, in the first iteration, the channel matrix $\mathbf{H}_0$ is randomly initialized. Equation. 18 is then used to recover the data modulation matrix $\hat{\mathbf{S}}_1$. Substituting the computed data modulation matrix $\hat{\mathbf{S}}_1$ to Eq. 19, the updated channel matrix $\hat{\mathbf{H}}_1$ can then be obtained. The channel matrix $\hat{\mathbf{H}}_i$ and the data modulation matrix $\hat{\mathbf{S}}_i$ is then repeatedly computed with increasing iteration number until the stopping condition is satisfied. In this paper, it is assumed that the data modulation matrix is successfully recovered when the error between the received signal and its reconstructed version from the estimated channel and data modulation matrices does not significantly change between two successive iterations i and $i+1$. Therefore, the stopping condition is represented by:

$$|e_{i+1} - e_i| \leq 10^{-5} \tag{20}$$

Algorithm 1: Semi-Blind Receiver Model Based on ALS.

Input:

The received tensor signal, $\widetilde{\mathcal{Y}}$;
The value of antenna allocation matrix, $\mathbf{A}$;
The value of frequency encoding matrix, $\mathbf{C}$;
The value of frequency assignation matrix, $\mathbf{U}$;

1: Let $i = 0$. Randomly initialize the channel matrix $\mathbf{H}_0$;
2: $i = i + 1$;
3: Compute the data modulation matrix $\hat{\mathbf{S}}_i$ via Eq. 18;
4: Compute the channel matrix $\hat{\mathbf{H}}_i$ via Eq. 19;
5: Loop through step 2 to step 4 until Eq. 20 is satisfied;

Output:

Data modulation matrix $\hat{\mathbf{S}}$, channel matrix $\hat{\mathbf{H}}$, and iteration number i;

where $e_i = \|\widetilde{\mathbf{Y}}_3 - (\mathbf{Q} \diamond \mathbf{P})\hat{\mathbf{S}}_i^{\mathrm{T}}\|_{\mathrm{F}}$ is the estimation error calculated at the i-th iteration of the ALS algorithm. If the estimation error is satisfied by Eq. 20, it is assumed that the ALS algorithm has converged at the i-th iteration.

The detailed process of the proposed semi-blind receiver algorithm is provided in Algorithm 1.

V. Identifiability and Uniqueness

In this section, identifiability and uniqueness issues in the proposed framework are discussed according to the recovering data modulation matrix and channel matrix by the proposed semi-blind ALS receiver.

A. Identifiability

Generally speaking, the notion identifiability in communication system design implies that the transmitted information can be reliably extracted from the received waveform. In the least squares (LS) sense, it linked to the recovery of $\hat{\mathbf{H}}$ and $\hat{\mathbf{S}}$ from $\mathbf{Y}_2$ and $\mathbf{Y}_3$, defined in Eq. (17) and Eq. (15), respectively. According to Eq. (17) and Eq. (15), the mathematical formulation of semi-blind ALS receiver given by Eq. (18) and Eq. (19) can be obtained. However, it should be noted that in order to obtain $\hat{\mathbf{H}}$ and $\hat{\mathbf{S}}$, left pseudo-inverse operations must be performed. It is known that left pseudo-inverse can not be always calculated, so identifiability can be considered as a condition of left pseudo-inverse.

By defining $\mathbf{Z}_2 = ((\mathbf{U} \odot \mathbf{C})^{\mathrm{T}} \diamond \mathbf{S})\mathbf{A}^{\mathrm{T}} \in \mathbb{C}^{NF \times M}$ and $\mathbf{Z}_3 = (\mathbf{HA}) \diamond (\mathbf{U} \odot \mathbf{C})^{\mathrm{T}} \in \mathbb{C}^{FK \times R}$, these two expressions can be substituted into Eq. 17 and Eq. 15, to obtain Eq. 21 and Eq. 22:

$$\mathbf{Y}_2 = ((\mathbf{U} \odot \mathbf{C})^{\mathrm{T}} \diamond \mathbf{S})\mathbf{A}^{\mathrm{T}}\mathbf{H}^{\mathrm{T}} = \mathbf{Z}_2\mathbf{H}^{\mathrm{T}} \tag{21}$$

$$\mathbf{Y}_3 = ((\mathbf{HA}) \diamond (\mathbf{U} \odot \mathbf{C})^{\mathrm{T}})\mathbf{S}^{\mathrm{T}} = \mathbf{Z}_3\mathbf{S}^{\mathrm{T}} \tag{22}$$

Theorem 1 (Identifiability): Supposing $\mathbf{H}$ and $\mathbf{S}$ have full column-rank, identifiability of $\mathbf{H}$ and $\mathbf{S}$ from Eq. 21 and Eq. 22 respectively requires that $\mathbf{Z}_2$ and $\mathbf{Z}_3$ are full column-rank which satisfy:

$$\begin{aligned} rank(\mathbf{Z}_2) &= M \\ rank(\mathbf{Z}_3) &= R \end{aligned} \tag{23}$$

Proof 1: The assumption of the full column-rank of data modulation matrix $\mathbf{S} \in \mathbb{C}^{N \times R}$ and channel matrix $\mathbf{H} \in \mathbb{C}^{K \times M}$, which implies $N \geq R$ and $K \geq M$, is reasonable. The values of the two matrices are linear independent because they are randomly drawn from PSK/QAM alphabets and MIMO fading coefficients. The number of receiving antennas is set as no less than the transmitting antennas, and the length of user symbols is set no less than the number of users. Therefore, the condition for the full column-rank of data modulation matrix and channel matrix can be guaranteed. From Eq. 21, $\mathbf{H}$ is identifiable in the LS sense only if $\mathbf{Z}_2 \in \mathbb{C}^{NF \times M}$ permits a unique left pseudo-inverse, meaning that $\mathbf{Z}_2$ is full column-rank to recover $\hat{\mathbf{H}}$. This the theorem of left pseudo-inverse in the matrix theory. Applying the same reasoning to $\mathbf{S}$ in Eq. 22 will illustrate that $\mathbf{Z}_3 \in \mathbb{C}^{FK \times R}$ is full column-rank. ■

According to Theorem 1 it is known that the necessary and sufficient condition for the identifiability of recovering data modulation matrix $\mathbf{S}$ and channel matrix $\mathbf{H}$ is the full column-rank property of $\mathbf{Z}_2$ and $\mathbf{Z}_3$. In Theorem 2, a necessary (but not sufficient) condition for identifiability is provided.

Theorem 2: Assume that $\mathbf{H}$ and $\mathbf{S}$ have full column-rank. The necessary (but not sufficient) condition for identifiability is that $\mathbf{Z}_2$ and $\mathbf{Z}_3$ are "tall" matrices, which implies:

$$NF \geq M, \quad FK \geq R \tag{24}$$

The inequalities can be viewed as restrictions when designing the values of parameters (N, F, M, K, R).

B. Uniqueness

According to the discussion of identifiability, the data modulation matrix $\mathbf{S}$ can be recovered and channel matrix $\mathbf{H}$ can be estimated by satisfying the necessary and sufficient condition in Theorem 1. Whether the recovery matrices are unique must also be considered. In this section, uniqueness as corresponding to the recovery data modulation matrix $\mathbf{S}$ and channel matrix $\mathbf{H}$ is discussed, and the concept of k-rank as represented by Kruskal is introduced [41].

Definition 1: Consider the matrix $\mathbf{A} \in \mathbb{C}^{I_1 \times I_2}$. The rank$(\mathbf{A}) = t$ means there are t linearly independent columns in the matrix $\mathbf{A}$. If every $l \leq I_2$ column of $\mathbf{A}$ is linearly independent, but l + 1 columns are linearly dependent, then the k-rank of $\mathbf{A}$ is l, which can be denoted as $k_{\mathbf{A}} = l$.

Next, k-rank is used to describe the theorem of uniqueness of a 3rd-order PARAFAC decomposition model. The frontal slice of a 3rd-order tensor $\mathcal{X} \in \mathbb{C}^{I \times J \times K}$ is denoted by $\mathbf{X}_{..k} = \mathbf{A}diag(\mathbf{c}_{k.})\mathbf{B}^{\mathrm{T}}$. The condition of uniquely recovering the three component matrices is then denoted by Theorem 3.

Theorem 3: [42] Given a frontal slice $\mathbf{X}_{..k} = \mathbf{A}diag(\mathbf{c}_{k.})\mathbf{B}^{\mathrm{T}}$ of a 3rd-order tensor $\mathcal{X} \in \mathbb{C}^{I \times J \times K}$, where $\mathbf{A} \in \mathbb{C}^{I \times R}$, $\mathbf{B} \in \mathbb{C}^{J \times R}$, and $\mathbf{C} \in \mathbb{C}^{K \times R}$, if

$$k_{\mathbf{A}} + k_{\mathbf{B}} + k_{\mathbf{C}} \geq 2(R + 1) \tag{25}$$

then the three component matrices $\mathbf{A}$, $\mathbf{B}$, and $\mathbf{C}$ are unique up to permutation and (complex) scaling of columns.

Theorem 3 is a promotion form of the theorem in the seminal paper [41] from real ($\mathbb{R}$) to complex ($\mathbb{C}$) domain. Note that

permutation ambiguity and scaling ambiguity exists between the original information and recovery information, and this will be discussed in following section. By using Theorem 3, the condition of uniqueness in the proposed framework to recover the data modulation matrix $\mathbf{S}$ and the channel matrix $\mathbf{H}$ is explored. Note that the condition in Theorem 3 is used to recover all three component matrices, but only two estimated matrices are required in the proposed framework. Thus, the condition is more strict and can be understood as sufficient but not necessary in the proposed framework.

Theorem 4: As $\mathbf{Q} = \mathbf{HA}$ and $\mathbf{P} = (\mathbf{U} \odot \mathbf{C})^{\mathrm{T}}$ have been defined, the Eq. 14 can be written as:

$$\mathcal{Y}_{\cdot\cdot n} = \mathbf{Q} diag(\mathbf{s}_{n\cdot}) \mathbf{P}^{\mathrm{T}} \tag{26}$$

It can be seen that this formulation is familiar with the frontal slice in Theorem 3. Therefore, supposing that, $\mathbf{Q} \in \mathbb{C}^{K \times R}$, $\mathbf{S} \in \mathbb{C}^{N \times R}$, and $\mathbf{P} \in \mathbb{C}^{F \times R}$ are full k-rank, then according Eq. 25, it will yield:

$$\min(K, R) + \min(N, R) + \min(F, R) \geq 2(R + 1) \tag{27}$$

The proof of Theorem 4 is similiar with the process of the seminal paper [42]. When the parameters (K, R, N, F) in the T-HoCWD framework are satisfied with Theorem 4, unique $\mathbf{Q} = \mathbf{HA}$, $\mathbf{S}$, and $\mathbf{P} = (\mathbf{U} \odot \mathbf{C})^{\mathrm{T}}$ matrices can be obtained up to the permutation and scaling ambiguity, which can be eliminated. In the T-HoCWD framework, it is assumed that the matrix $\mathbf{P} = (\mathbf{U} \odot \mathbf{C})^{\mathrm{T}}$ and the antenna allocation matrix $\mathbf{A}$ are known by the receiver. All that is required is semi-blindly recovering the data modulation matrix $\mathbf{S}$ and the channel matrix $\mathbf{H}$. According to the work of A.L.De Almeida [43], it is known that phase and scale ambiguities exist, but there is no permutation ambiguity. Thus, the recovery matrices can be denoted by:

$$\hat{\mathbf{S}} = \alpha \mathbf{S}, \quad \hat{\mathbf{H}} = 1/\alpha \mathbf{H} \tag{28}$$

where $\hat{\mathbf{S}}$ and $\hat{\mathbf{H}}$ are the matrices recovered by the proposed semi-blind receiver in Section III, and α is the scaling ambiguity factor. To eliminate the ambiguities, few known sequences are added to compute the value of α. Herein, it is assumed that the first symbol $s_{1,1}$ of the data modulation matrix $\mathbf{S}$ is known, then Eq. (28) can be used to compute the value of α.

VI. Simulation Results

A set of computer simulation results are presented to analyze the performance of the proposed framework for various configurations with the ideal receiver. The performance of the proposed semi-blind receiver compared with the ideal receiver is then demonstrated. The semi-blind ALS receiver avoids using a lot of pilot sequences, but relies on the knowledge of the first value of the data modulation matrix $\mathbf{S}$ for eliminating scaling ambiguities, as denoted by Eq. (28). The goals of the following experiments include: i) To evaluate the proposed T-HoCWD framework having identical bit-error-rate (BER) performance with the SMSE model; ii) To verify that the proposed H-ToCWD model can work well under MIMO systems, comparing the BER performance of the proposed model to the existing Alamouti coding methods [44] and maximum ratio combining (MRC) algorithm [45]; iii) To show the convergence of the proposed semi-blind ALS receiver and performances compared with the ideal receiver.

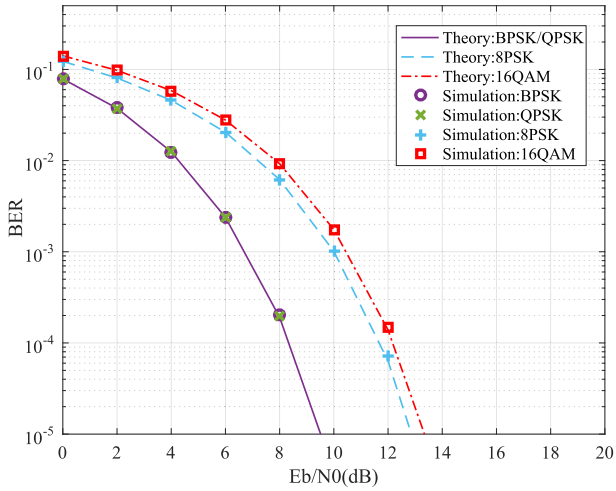

Fig. 5. BER performance of the OFDM waveform generated by the proposed framework in the AWGN channel under a SISO system.

The results represent an average of 2,000 Monte Carlo runs. At each run, the MIMO channel is Rayleigh distributed which is time-invariant and flat fading. The bit error rate(BER) curves are plotted as a function of the energy per bit to noise power spectral density ratio (Eb/N0). The additive noise power is fixed according to the desired signal to noise ratio (SNR) given by:

$$\mathrm{SNR(dB)} = 10\log_{10} \frac{\|\mathcal{X}\|_{\mathrm{F}}^2}{\|\mathcal{N}\|_{\mathrm{F}}^2} \tag{29}$$

where $\mathcal{N}$ is an additive noise tensor whose entries are drawn from complex-valued Gaussian distribution with zero-mean and unit variance. The relationship between SNR and Eb/No is represented by:

$$\mathrm{Eb/N0(dB)} = \mathrm{SNR(dB)} + 10\log_{10} \frac{W}{R_b} \tag{30}$$

where W and R_b denote the bandwidth and bit rate, respectively.

A. BER Performance Under a SISO System With the ZF Receiver

The performance of the proposed framework is initially evaluated under a single-input single-output (SISO) system. In this case, the framework can be seen as a SMSE model. The ideal receiver for recovering the transmitted symbols is used, as given by Eq. (16), and the parameters $M = K = 1$ are set to obtain a SISO system. It is assumed that it is single user system, meaning that $R = 1$. There are 128 sub-carriers ($F = 128$) that are partly utilized by each user without any frequency encoding. In this case, an OFDM waveform is generated in the transmitter. The BER performance of the OFDM waveform generated by the proposed model is illustrated in Fig. 5, and compared with theory curves under the additive white gaussian noise (AWGN) channel. When selecting the values of frequency encoding matrix $\mathbf{C}$ from the Hadamard matrix, the MC-CDMA waveform can be

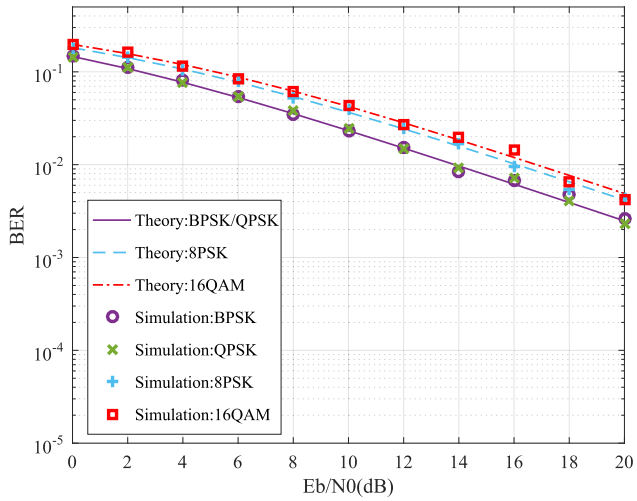

Fig. 6. BER performance of the MC-CDMA waveform generated by the proposed framework in the Rayleigh channel under a SISO system.

obtained. Fig. 6 shows the BER performance of the MC-CDMA waveform generated by the proposed model in a Rayleigh channel. When the values of the data modulation matrix $\mathbf{S}$ are altered, different kinds of modulated signals are obtained such as BPSK/QPSK/8PSK/16QAM. It can be observed that the BER performances of these signals are same as theoretical curves from the simulation results. These findings are consistent with the results of [8], proveing that the proposed model can achieve the function of the SMSE model. The variable configurations of implementing OFDM and MC-CDMA waveforms in this experiment are summarized in Table III. The matrix $\mathbf{A} = [1]$ denotes that there is only one user symbol transmitted by the transmitting antenna.

B. BER Performance Under MIMO System With ZF Receiver

In this sub-section, the performance of the proposed framework under MIMO systems is tested, and also contains perfect channel knowledge.

1) Different Antenna Configurations: The number of transmitting and receiving antennas are altered to analyze the BER performance compared to the existing Alamouti encoding schemes and the maximum-ratio combining (MRC) method. It is alse assumed that there are two users ($R = 2$) and 128 sub-carriers ($F = 128$). The sub-carriers are partly used by the two users without frequency encoding, meaning the OFDM waveform is generated. The modulation method is quadrature phase shift keying (QPSK). The result of setting up different numbers of transmitting and receiving antennas is shown in Fig. 7. According to the simulation results, it can be seen that performance is not improved when only adding the number of transmitted antennas. This is because the proposed model does not include space-time encoding. Adding transmitting antennas will only bring a gain in space diversity which will increase the rate of transmitting signals in the MIMO wireless communication system. However, when adding the number of receiving antennas, perfect performance can be achieved with

TABLE III
VARIABLE CONFIGURATIONS OF IMPLEMENTING OFDM AND MC-CDMA WAVEFORMS BY THE PROPOSED FRAMEWORK IN A SISO SYSTEM

Operations	OFDM	MC-CDMA
Data modulation	PSK/QAM	PSK/QAM
Frequency encoding	None	Hadamard
Frequency assignation	Partly assigned	Partly assigned
Antenna allocation	$\mathbf{A} = [1]$	$\mathbf{A} = [1]$
Channel	AWGN	Rayleigh

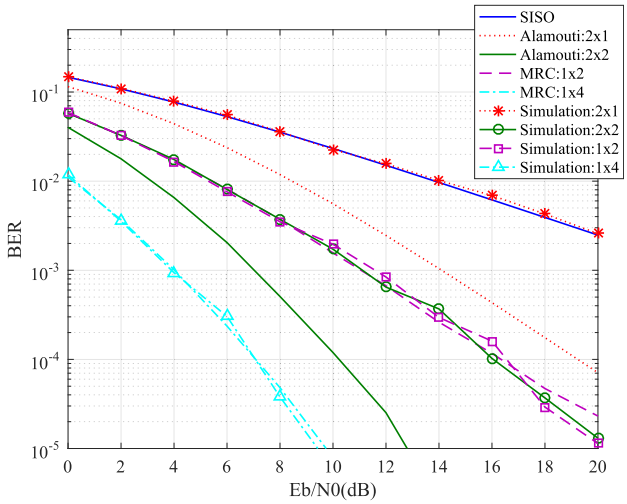

Fig. 7. BER performance of the proposed model with different antenna configurations compared to some existing methods in the Rayleigh channel.

TABLE IV
VARIABLE CONFIGURATIONS OF IMPLEMENTING OFDM AND MC-CDMA WAVEFORMS BY THE PROPOSED FRAMEWORK IN A MIMO SYSTEM

Operations	OFDM	MC-CDMA
Data modulation	PSK/QAM	PSK/QAM
Frequency encoding	None	Hadamard
Frequency assignation	Partly assigned	Partly assigned
Antenna allocation	$\mathbf{A} = [1 \quad 0; 0 \quad 1]$	$\mathbf{A} = [1 \quad 1]$
Channel	2×2 Rayleigh	1×4 Rayleigh

MRC method which is the optimal idea to solve the multiple receiving antennas combination problem. As the number of receiving antennas increases, the BER performance improves.

2) Different Kinds of Data Modulation and Frequency Encoding Methods: The simulation conditions of this experiment are summarized in Table IV. The matrix $\mathbf{A} = [1 \quad 0; 0 \quad 1]$ in this table shows that each user is utilizing a single antenna to transmit symbols. The proposed framework is first used to generate the OFDM waveform in a MIMO system with two transmitting antennas ($M = 2$) and two receiving antennas ($K = 2$). There

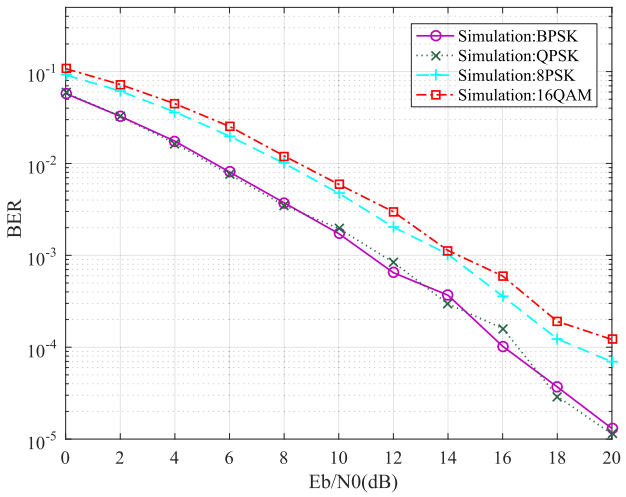

Fig. 8. BER performance of the OFDM waveform generated by the proposed framework with different data modulation matrices in a MIMO (2 × 2) system.

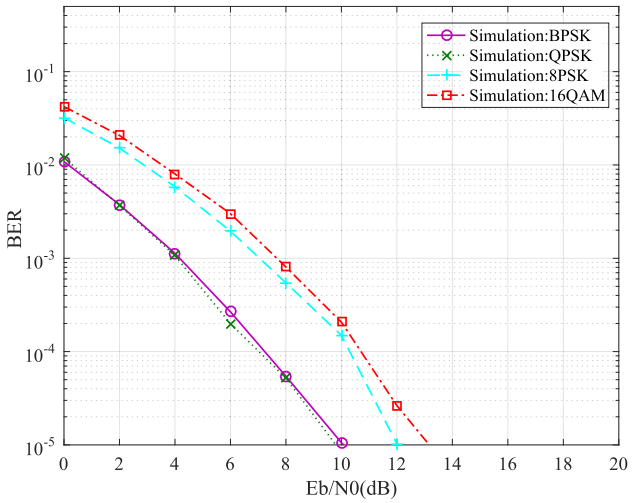

Fig. 9. BER performance of the MC-CDMA waveform generated by the proposed framework with different data modulation matrices in a MIMO (1 × 4) system.

are 128 sub-carriers ($F = 128$) partly used by two users ($R = 2$) without frequency encoding. Different kinds of OFDM modulated signals can be obtained by altering the data modulation matrix. The MC-CDMA waveform is then generated by adding frequency encoding to the former simulation conditions in a MIMO system with one transmitting antenna ($M = 1$) and four receiving antennas ($K = 4$). The values of the frequency encoding matrix $\mathbf{C}$ are selected from the Hadamard matrix. Botn Fig. 8 and Fig. 9 illustrate that the proposed framework can achieve the function of transmitting different multi-carrier signals in a MIMO system, while the SMSE model can not.

3) Different Kinds of Frequency Assignation: One of the advantages of the CR is the ability to adjust the spectrum in use by sensing results to avoid interference and improve spectrum utilization. Thus, frequency assignment performance in the proposed framework is very important if it is to be used in

TABLE V
FOUR METHODS OF FREQUENCY ASSIGNATION IN A MIMO (1 × 2) SYSTEM

Method1	$\mathbf{U} = \begin{bmatrix} \text{zeros}(1,64) & \text{ones}(1,16) & \text{zeros}(1,48) \\ \text{zeros}(1,48) & \text{ones}(1,16) & \text{zeros}(1,64) \end{bmatrix}$
Method2	$\mathbf{U} = \begin{bmatrix} \text{zeros}(1,112) & \text{ones}(1,16) \\ \text{ones}(1,16) & \text{zeros}(1,112) \end{bmatrix}$
Method3	$\mathbf{U} = \begin{bmatrix} \text{zeros}(1,24) & \text{ones}(1,16) & \text{zeros}(1,88) \\ \text{zeros}(1,88) & \text{ones}(1,16) & \text{zeros}(1,24) \end{bmatrix}$
Method4	$\mathbf{U} = \begin{bmatrix} \text{zeros}(1,16) & \text{ones}(1,32) & \text{zeros}(1,80) \\ \text{zeros}(1,96) & \text{ones}(1,16) & \text{zeros}(1,16) \end{bmatrix}$

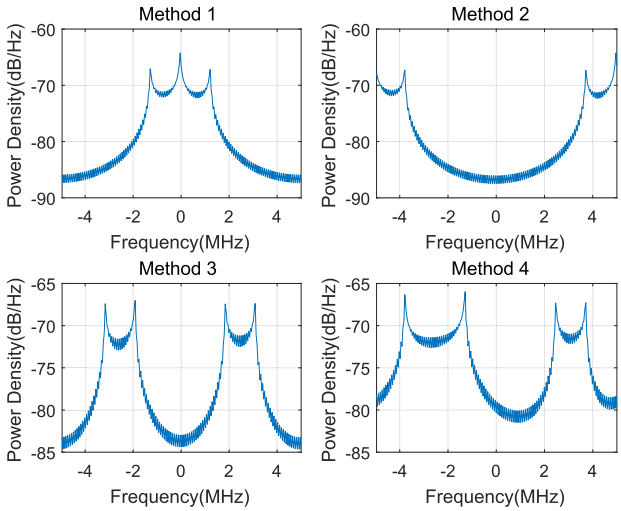

Fig. 10. The power density diagram when changing the methods of frequency assignation in a MIMO (1 × 2) system.

a SDR platform and in DSA technology. In this numerical simulation, the methods of assigning frequencies to users in a MIMO system are altered to evaluate the performance of frequency assignment in the proposed framework. The four methods are summarized in Table V. The frequency assignment matrix $\mathbf{U}$ is denoted in the form of Matlab, where zeros (1, 64) denote the number of 0's is 64, and ones (1, 16) denote the number of 1's is 16. In a MIMO system with one transmitting antenna ($M = 1$) and two receiving antennas ($K = 2$), it is assumed that there are 128 sub-carriers ($F = 128$) which are assigned to two users ($R = 2$) without frequency encoding. The different methods to assign frequency are illustrated Fig. 10, and Fig. 11 shows the corresponding BER curves. The two simulation results illustrate that the proposed framework can achieve the function of changing frequency assignation and that different methods of frequency assignation do not influence the BER performance of the MIMO system.

4) Different Numbers of Users: The question of whether BER performance will decrease as the number of users increase must be considered in a multi-user system. It also must be determined if there is interference among users or not. In this experiment, the BER performance of the proposed framework is tested while increasing the number of users. A MIMO system equipped with two transiting antennas ($M = 2$) and four receiving antennas ($K = 4$) is used, and the user symbols are

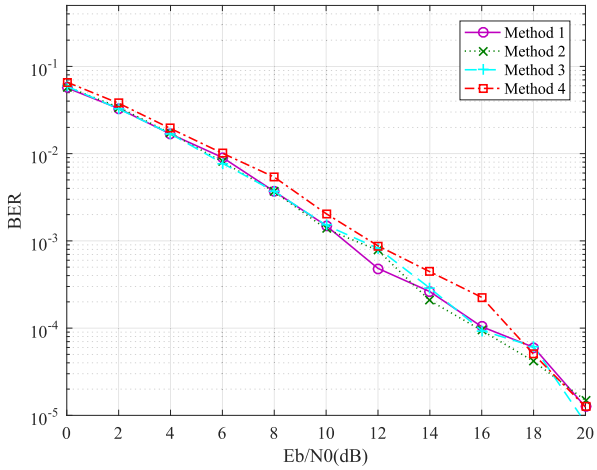

Fig. 11. BER performance of different methods of frequency assignation in a MIMO (1×2) system.

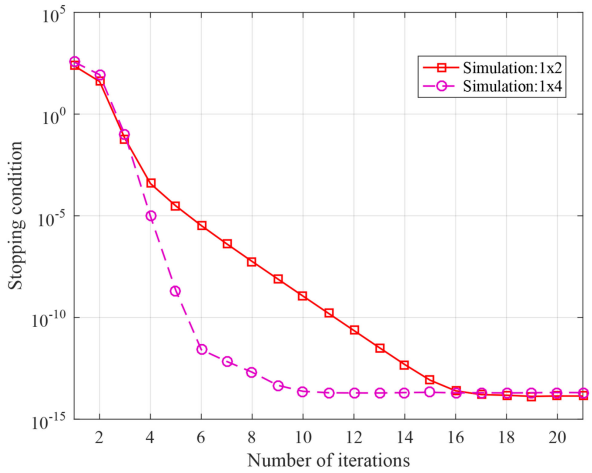

Fig. 13. Convergence performance of the proposed semi-blind receiver with different antenna configurations.

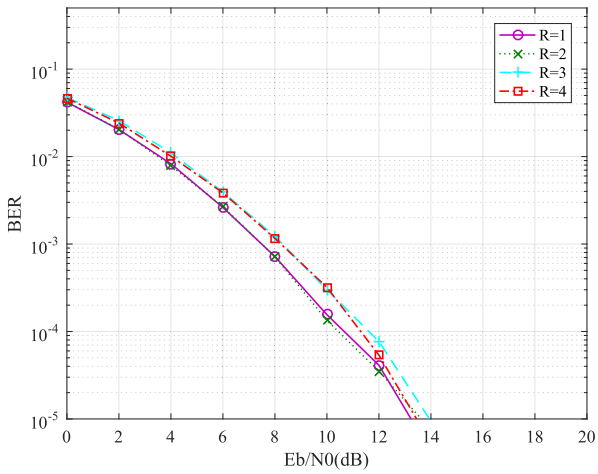

Fig. 12. The performance of the proposed framework with different numbers of users in a MIMO (2×4) system.

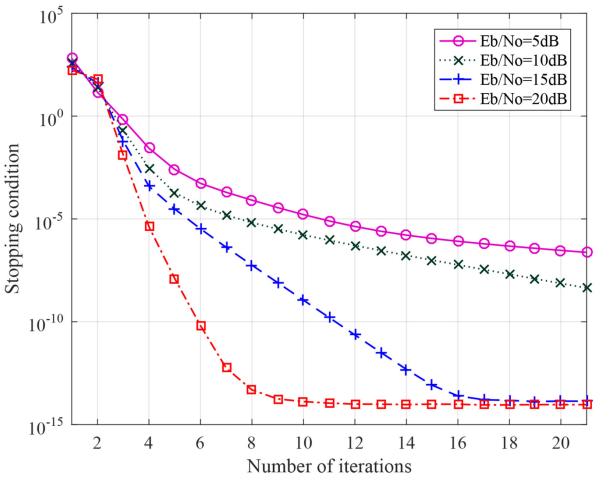

Fig. 14. Convergence performance of the proposed semi-blind receiver with different values of Eb/No in a MIMO (1×2) system.

drawn from 16QAM alphabets. Every user will use a different 32 sub-carriers from the available 128 sub-carriers. The simulation result is provided in Fig. 12. Findings show that when the number of users is increased, the BER performance of the system does not decline, meaning that different users will not interfere with each other.

C. BER Performance With Semi-Blind ALS Receiver

In this section, experiments are carried out to examine the behaviors of the proposed semi-blind ALS receiver.

1) Evaluation of the Convergence: The convergence performance of the proposed semi-blind ALS algorithm is first evaluated. Fig. 13 shows the relationship between the stopping condition and the number of iterations. The stopping condition refers to the situation that the difference between the two error functions is less than or equal to 10^{-5}, as is shown in Eq. 20. The error function refers to the difference between the received signal and the actual received signal estimated by the ALS demodulation algorithm and the data modulation variable and the channel state information matrix, as denoted by: $e_i = \|\widetilde{\mathbf{Y}}_3 - (\mathbf{Q} \diamond \mathbf{P})\hat{\mathbf{S}}_i^{\mathrm{T}}\|_{\mathrm{F}}$. In this experiment, a MIMO system with one transmitting antenna ($M = 1$) and two receiving antennas ($K = 2$) is used. There are also 128 sub-carriers ($F = 128$) which are partly used by the two users ($R = 2$). Simulation results illustrate that when the values of Eb/No increase, the number of iterations decline under the same error value. Fig. 14 illustrates the convergence performance of demodulation algorithm for the semi-blind receiver when the number of receiving antennas is changed under Eb/No equal to 15 dB. Note that the number of iterations declines with an increasing number of receiving antennas. However, at least three iterations are required to meet the convergence conditions, as denoted by Eq. (20).

2) Performance of Symbol Recovery Based on the Semi-Blind Receiver: The proposed semi-blind ALS receiver can jointly recover user symbols and channel information without using sequences. The BER performance in recovering user symbols

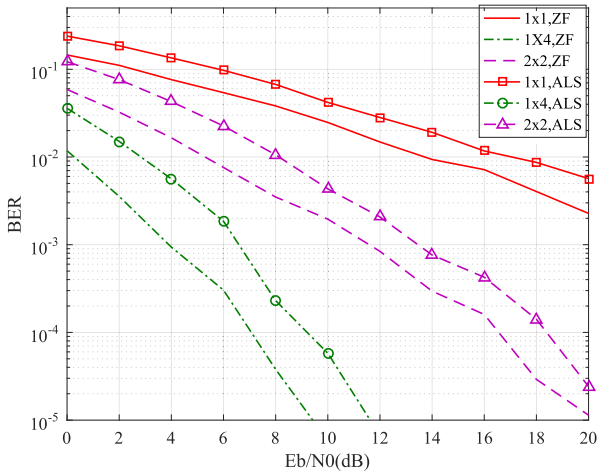

Fig. 15. BER performance of the proposed semi-blind receiver with different antenna configurations in the Rayleigh channel.

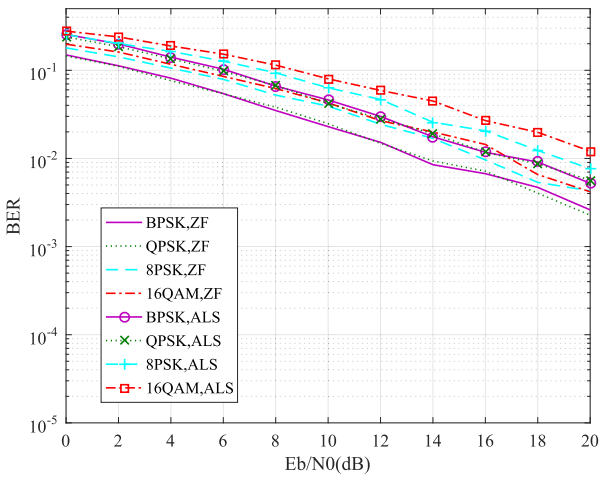

Fig. 16. BER performance of the proposed semi-blind receiver with various data modulation matrices in the Rayleigh channel.

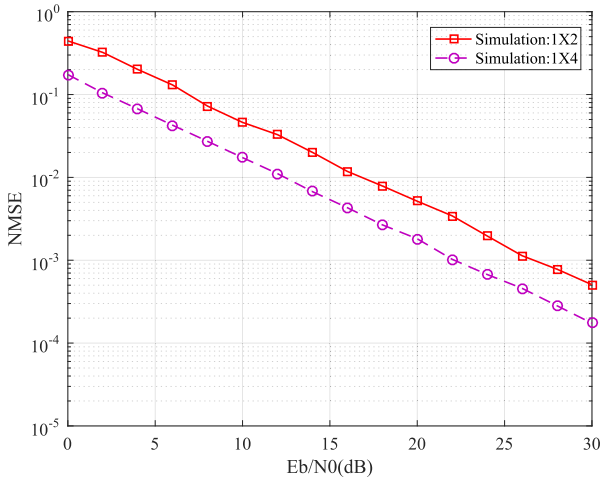

Fig. 17. The NMSE performance of channel estimation by the proposed semi-blind ALS receiver.

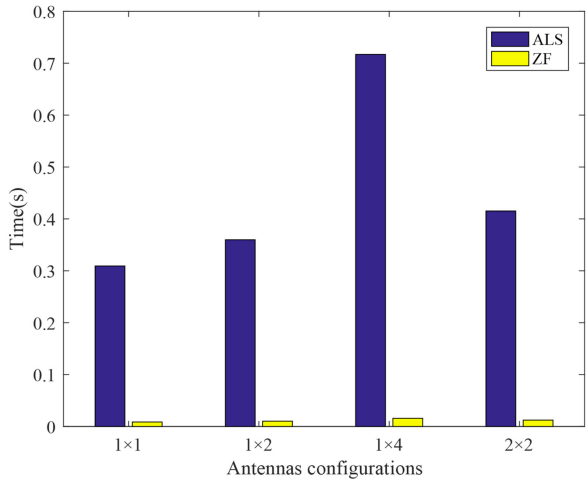

Fig. 18. Simulation time of ALS receiver with different antenna configurations compared to ZF receiver under QPSK modulation.

using the semi-blind ALS receiver is therefore investigated and compared with the ideal receiver. In this experiment, 128 sub-carriers ($F = 128$) are partly used by the two users ($R = 2$). Fig. 15 shows the performance of the ALS receiver compared to the zero-forcing (ZF) receiver by configuring different numbers of antennas. The modulation method is QPSK. In Fig. 16, the result with various modulated methods in a SISO system is provided. It can be seen from the two simulation results that the gap between the ALS and ZF receiver is around 3 dB in terms of Eb/No. It can also be observed that the same performance improvement is obtained for both ZF and ALS receivers when the Eb/No is increased.

3) Performance of Channel Estimation Based on the Semi-Blind Receiver: The proposed semi-blind ALS receiver performance in estimating channel information is next reviewed. The normalized mean square error (NMSE) as represented by Eq. (31), is used here to evaluate the accuracy of channel estimation by the ALS receiver:

$$\mathrm{NMSE}(\mathbf{H}) = \frac{\|\hat{\mathbf{H}}_i - \mathbf{H}\|_{\mathrm{F}}^2}{\|\mathbf{H}\|_{\mathrm{F}}^2} \tag{31}$$

where $\hat{\mathbf{H}}_i$ denotes the recovery channel matrix which is estimated by the i-th iteration. The results of channel estimation by the proposed semi-blind ALS receiver are provided in Fig. 17. The values of NMSE can be seen to linearly decrease with the increasing of Eb/No. It can also be observed that when changing the number of receiving antennas from two to four, the value of Eb/No decreases by nearly 5 dB with the same NMSE.

4) Complexity Comparison: The complexity of the proposed semi-blind ALS receiver is compared with ZF receiver. The simulation time of ALS receiver is longer than ZF receiver, because it does not require long training sequences and channel estimates. In this experiment, 128 subcarriers (F = 128) are partly used by the two users (R = 2). The simulation time of

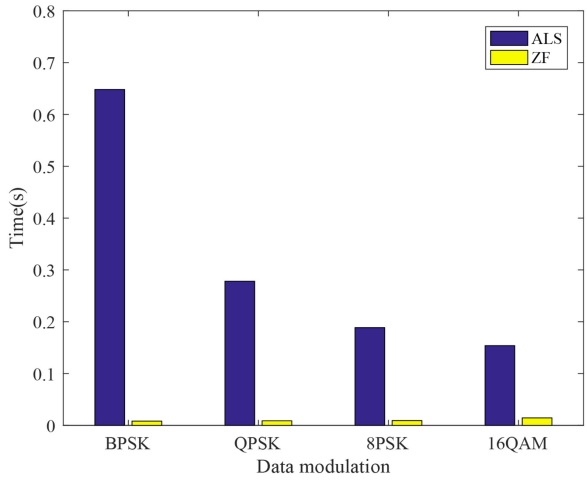

Fig. 19. Simulation time of ALS receiver with different modulation methods compared to ZF receiver in a SISO system.

ALS and ZF receivers with different antenna structures and modulation modes is compared. In each case, the simulation result takes the average time of 1000 simulations. The simulation time of ALS receiver with different antenna configurations compared to ZF receiver are provided in Fig. 18. The modulation method is QPSK. The proposed semi-blind ALS receiver requires more simulation time because it does not know the channel information. Matrix operations also increase the simulation time. In Fig. 19, the simulation time of ALS receiver with different modulation methods compared to ZF receiver in a SISO system is provided. Similarly, the simulation time of ALS is much longer than that of ZF under different modulation methods.

VII. Conclusion

In this paper, a new analytic framework was proposed to generate different kinds of multi-carrier waveforms by choosing corresponding values of the four variables for a MIMO system. The new framework can be seen as an extension of the SMSE framework which can realize the functions of SMSE, and also can work well in a MIMO system, where the SMSE framework can not. Two kinds of tensor decomposition models, PARAFAC and TUCKER-1, were used to model the proposed framework. Specifically, the core tensor of TUCKER-1 was altered by PARAFAC model. Because of the performance of tensor decomposition models, the proposed framework is guaranteed to experience identifiability and uniqueness issues. A new semi-blind ALS receiver was also presented in this paper for use in the proposed model. The new receiver can recover user symbols and estimate channel state information without using many pilot sequences, increasing the rate of transmitting signals. Compared with the ideal receiver, the performance of the proposed semi-blind receiver decreased by approximately 3 dB. Performance simulation results illustrated that the proposed framework and the semi-blind ALS receiver can be successfully implemented in an SDR platform and DSA technology.

The following work needs to be further studied in the future. On the one hand, MIMO space-time frequency coding is not introduced into the proposed model. This makes the communication performance of the system not as good as that of classical Alamouti coding. Therefore, the model should be further extended in the subsequent research, so that the system can include space, time, frequency and other coding methods. On the other hand, modulation pattern recognition is not considered in the proposed semi-blind receiver. Modulation pattern recognition is a necessary means to achieve blind receiver in cognitive radio. In the subsequent research, the author of this paper will carry out modulation pattern recognition in combination with semi-blind receiver.

References

[1] F. K. Jondral, "Software-defined radio: Basics and evolution to cognitive radio," *EURASIP J. Wireless Commun. Netw.*, vol. 2005, no. 3, pp. 275–283, 2005.

[2] I. F. Akyildiz, W. Y. Lee, M. C. Vuran, and S. Mohanty, "Next generation/dynamic spectrum access/cognitive radio wireless networks: A survey," *Comput. Netw.*, vol. 50, no. 13, pp. 2127–2159, 2006.

[3] Y. Lin, C. Wang, J. Wang, and Z. Dou, "A novel dynamic spectrum access framework based on reinforcement learning for cognitive radio sensor networks," *Sensors*, vol. 16, no. 10, 2016, Art. no. 1675.

[4] C. R. Stevenson, G. Chouinard, Z. Lei, W. Hu, S. J. Shellhammer, and W. Caldwell, "IEEE 802.22: The first cognitive radio wireless regional area network standard," *IEEE Commun. Mag.*, vol. 47, no. 1, pp. 130–138, Jan. 2009.

[5] G. Scutari and D. P. Palomar, "MIMO cognitive radio: A game theoretical approach," *IEEE Trans. Signal Process.*, vol. 58, no. 2, pp. 761–780, Feb. 2010.

[6] H. Huang, J. Yang, Y. Song, H. Huang, and G. Gui, "Deep learning for super-resolution channel estimation and DOA estimation based massive MIMO system," *IEEE Trans. Veh. Technol.*, vol. 67, no. 9, pp. 8549–8560, Sep. 2018.

[7] S. Haykin, "Cognitive radio: Brain-empowered wireless communications," *IEEE J. Sel. Areas Commun.*, vol. 23, no. 2, pp. 201–220, Feb. 2005.

[8] M. L. Roberts, M. A. Temple, R. A. Raines, R. F. Mills, and M. E. Oxley, "Communication waveform design using an adaptive spectrally modulated, spectrally encoded (SMSE) framework," *IEEE J. Sel. Topics Signal Process.*, vol. 1, no. 1, pp. 203–213, Jun. 2007.

[9] Y. Tu, Y. Lin, J. Wang, and J. U. Kim, "Semi-supervised learning with generative adversarial networks on digital signal modulation classification," *Comput. Mater. Continua*, vol. 55, no. 2, pp. 243–254, 2015.

[10] K. Suto, H. Nishiyama, N. Kato, K. Mizutani, O. Akashi, and A. Takahara, "An overlay-based data mining architecture tolerant to physical network disruptions," *IEEE Trans. Emerg. Topics Comput.*, vol. 2, no. 3, pp. 292–301, Sep. 2014.

[11] H. Huang, Y. Peng, J. Yang, W. Xia, and G. Gui, "Fast beamforming design via deep learning," *IEEE Trans. Veh. Technol.*, vol. 69, no. 1, pp. 1065–1069, Jan. 2020.

[12] J. Sun, W. Shi, Z. Yang, J. Yang, and G. Gui, "Behavioral modeling and linearization of wideband RF power amplifiers using BiLSTM networks for 5G wireless systems," *IEEE Trans. Veh. Technol.*, vol. 68, no. 11, pp. 10 348–10 356, Nov. 2019.

[13] Z. Dou, G. Si, Y. Lin, and M. Wang, "An adaptive resource allocation model with anti-jamming in IoT network," *IEEE Access*, vol. 7, pp. 93 250–93 258, 2019.

[14] E. Like, M. Temple, and Z. Wu, "Soft decision design of spectrally partitioned CI-SMSE waveforms for coexistent applications," in *Proc. IEEE Int. Conf. Commun.*, 2010, pp. 1–6.

[15] M. Roberts, M. Temple, R. Mills, and R. Raines, "Interference suppression characterisation for spectrally modulated, spectrally encoded signals," *Electron. Lett.*, vol. 42, no. 19, pp. 1103–1104, 2006.

[16] M. L. Roberts, M. A. Temple, R. F. Mills, and R. A. Raines, "An SMSE implementation of CDMA with partial band interference suppression," in *Proc. IEEE Global Telecommun. Conf.*, 2007, pp. 4424–4428.

[17] V. Chakravarthy *et al.*, "Novel overlay/underlay cognitive radio waveforms using SD-SMSE framework to enhance spectrum efficiency—Part I: Theoretical framework and analysis in AWGN channel," *IEEE Trans. Commun.*, vol. 57, no. 12, pp. 3794–3804, Dec. 2009.

[18] P. Rose, R. Zhou, Y. Qu, V. Chakarvarthy, Z. Wu, and Z. Zhang, "Demonstration of hybrid overlay/underlay waveform generator with spectrally compliant cognitive capability via SD-SMSE framework," in *Proc. IEEE Annu. Consum. Commun. Netw. Conf.*, 2016, pp. 258–259.

[19] R. Zhou, X. Li, V. Chakarvarthy, and Z. Wu, "Software defined radio implementation of SMSE based overlay cognitive radio in high mobility environment," in *Proc. IEEE Global Telecommun. Conf.*, 2011, pp. 1–5.
[20] Y. Zhao, L. Qi, Z. Dou, and R. Zhou, "MIMO waveform design using spectrally modulated spectrally encoded (SMSE) framework," in *Proc. Int. Conf. Comput. Sci. Netw. Technol.*, 2016, pp. 688–691.
[21] Z. Dou, C. Li, C. Li, G. Si, and Q. Feng, "Framework on tensor modulated tensor encoded," in *Proc. IEEE Int. Conf. Electron. Inf. Commun. Technol.*, 2016, pp. 187–190.
[22] T. G. Kolda and B. W. Bader, "Tensor decompositions and applications," *SIAM Rev.*, vol. 51, no. 3, pp. 455–500, 2009.
[23] A. L. F. de Almeida, G. Favier, J. C. M. Mota, and J. da Costa, "Overview of tensor decompositions with applications to communications," in *Signals and Images: Advances and Results in Speech, Estimation, Compression, Recognition, Filtering, and Processing*, R. Coelho, V. Nascimento, R. de Queiroz, J. Romano, and C. Cavalcante, Eds., Boca Raton, FL, USA: CRC Press, 2016, pp. 325–356.
[24] A. L. De Almeida, G. Favier, and L. R. Ximenes, "Space-time-frequency (STF) MIMO communication systems with blind receiver based on a generalized paratuck2 model," *IEEE Trans. Signal Process.*, vol. 61, no. 8, pp. 1895–1909, Apr. 2013.
[25] G. Favier and A. L. de Almeida, "Tensor space-time-frequency coding with semi-blind receivers for MIMO wireless communication systems," *IEEE Trans. Signal Process.*, vol. 62, no. 22, pp. 5987–6002, Nov. 2014.
[26] L. R. Ximenes, G. Favier, A. L. de Almeida, and Y. C. Silva, "Parafac-paratuck semi-blind receivers for two-hop cooperative MIMO relay systems," *IEEE Trans. Signal Process.*, vol. 62, no. 14, pp. 3604–3615, Jul. 2014.
[27] L. R. Ximenes, G. Favier, and A. L. de Almeida, "Semi-blind receivers for non-regenerative cooperative MIMO communications based on nested PARAFAC modeling," *IEEE Trans. Signal Process.*, vol. 63, no. 18, pp. 4985–4998, Sep. 2015.
[28] W. Yi, Z. Wang, and J. Wang, "Multiple antenna wireless communication signal blind recovery based on PARAFAC decomposition," in *Proc. Int. Conf. Netw. Inf. Syst. Comput.*, 2015, pp. 137–140.
[29] Y. Bin, W. Fangqing, and L. Su, "Estimation of multipath parameters in wireless communications using noncircular PARAFAC algorithm," in *Proc. Int. Symp. Antennas, Propag. EM Theory*, 2016, pp. 612–616.
[30] G. T. de Araújo and A. L. de Almeida, "Closed-form channel estimation for MIMO space–time coded systems using a fourth-order tensor-based receiver," *Circuits, Syst., Signal Process.*, vol. 37, no. 3, pp. 1343–1357, 2018.
[31] F. Wen and C. Liang, "Improved tensor-mode based direction-of-arrival estimation for massive MIMO systems," *IEEE Commun. Lett.*, vol. 19, no. 12, pp. 2182–2185, Dec. 2015.
[32] R. Boyer and M. Haardt, "Noisy compressive sampling based on block-sparse tensors: Performance limits and beamforming techniques," *IEEE Trans. Signal Process.*, vol. 64, no. 23, pp. 6075–6088, Dec. 2016.
[33] B. Mao *et al.*, "A tensor based deep learning technique for intelligent packet routing," in *Proc. IEEE Global Commun. Conf.*, 2017, pp. 1–6.
[34] F. Tang, B. Mao, Z. Md. Fadlullah, J. Liu, and N. Kato, "On extracting the spatial-temporal features of network traffic patterns: A tensor based deep learning model," in *Proc. Int. Conf. Netw. Infrastructure Digit. Content*, 2018, pp. 445–451.
[35] M. Tang, G. Ding, Z. Xue, J. Zhang, and H. Zhou, "Multi-dimensional spectrum map construction: A tensor perspective," in *Proc. Int. Conf. Wireless Commun. Signal Process.*, 2016, pp. 1–5.
[36] S. A. Cheema, Y. Evdokimov, M. Haardt, K. Naskovska, and B. Valeev, "Iterative GFDM receiver based on the paratuck2 tensor decomposition," in *Proc. Int. ITG Workshop Smart Antennas*, 2017, pp. 1–7.
[37] Z. Luo, L. Zhu, and C. Li, "Vandermonde constrained tensor decomposition based blind carrier frequency synchronization for OFDM transmissions," *Wireless Pers. Commun.*, vol. 95, no. 3, pp. 3459–3475, 2017.
[38] M. N. da Costa, G. Favier, and J. Romano, "Tensor modelling of MIMO communication systems with performance analysis and Kronecker receivers," *Signal Process.*, vol. 145, pp. 304–316, 2018.
[39] R. A. Harshman, "Foundations of the PARAFAC procedure: Models and conditions for an 'explanatory' multi-model factor analysis," *Ucla Work. Papers Phone.*, vol. 16, pp. 1–84, 1970.
[40] L. R. Tucker, "Some mathematical notes on three-mode factor analysis," *Psychometrika*, vol. 31, no. 3, pp. 279–311, 1966.
[41] J. B. Kruskal, "Three-way arrays: Rank and uniqueness of trilinear decompositions, with application to arithmetic complexity and statistics," *Linear Algebra Its Appl.*, vol. 18, no. 2, pp. 95–138, 1977.
[42] N. D. Sidiropoulos, G. B. Giannakis, and R. Bro, "Blind PARAFAC receivers for DS-CDMA systems," *IEEE Trans. Signal Process.*, vol. 48, no. 3, pp. 810–823, Mar. 2000.
[43] A. L. de Almeida, G. Favier, and J. C. M. Mota, "Constrained tensor modeling approach to blind multiple-antenna CDMA schemes," *IEEE Trans. Signal Process.*, vol. 56, no. 6, pp. 2417–2428, Jun. 2008.
[44] S. M. Alamouti, "A simple transmit diversity technique for wireless communications," *IEEE J. Sel. Areas Commun.*, vol. 16, no. 8, pp. 1451–1458, Oct. 1998.
[45] D. Brennan, "Linear diversity combining techniques," *Proc. IEEE*, vol. 91, no. 2, pp. 331–356, Feb. 2003.

Zheng Dou received the B.S. degree from Harbin Engineering University, Harbin, China, in 2001 and the Ph.D. degree from the College of Information and Communication Engineering, Harbin Engineering University, in 2007. He is currently a Professor with the College of Information and Communication Engineering, Harbin Engineering University. His research interests focus on the areas of intelligent wireless communication, cognitive radio and the design of communication signal waveform. Until now, he has presented more than 60 research papers, 20 patents, and three books. He was a Reviewer for several journals and conferences such as the IEEE COMMUNICATIONS, SIGNAL PROCESSING, IEEE ACCESS, *Journal of Communications*, and *Ship Engineering*. He has been a reviewer of National Natural Science Foundation and a senior member of China Communications Society.

Chunmei Li received the M.S. degree in communication engineering from Harbin Engineering University, Harbin, China, in 2019. Her research interests include machine learning and wireless communication.

Chao Li received the undergraduate and Ph.D. degrees from Harbin Engineering University, Harbin, China. He is currently with RIKEN Center on Advanced Intelligence Project, Tokyo, Japan. His research interests lie in the area of signal processing, machine learning, and applied mathematics. He has collaborated actively with researcher in several other disciplines, particularly neural computing and wireless communication.

Xiao Gao is currently working toward the M.S. degree in communication engineering from Harbin Engineering University, Harbin, China. Her research interests include deep learning, dynamic spectrum access, and wireless communications.

Lin Qi received the B.S. degree in communication engineering from Harbin Engineering University, Harbin, China, in 2002, the M.S. degree in signal and information processing from Harbin Engineering University, in 2005, and the Ph.D. degree in communication and information system from Harbin Engineering University, in 2011. From 2002 to 2005, she was an Assistant Professor of College of Information and Communication Engineering, Harbin Engineering University. Since 2007, she has been a Lecturer of College of Information and Communication Engineering, Harbin Engineering University. She also had been working with the Institute of Materials and Systems for Sustainability of Nagoya University from 2015 to 2016 as a Visiting Scholar. Her current research interests include wideband digital communication system, SDR, and communication signal processing.